Journal of Materials Research and Technology 28 (2024) 43–52

Contents lists available at ScienceDirect

Journal of Materials Research and Technology

journal homepage: www.elsevier.com/locate/jmrt

Atomic understanding of the evolutionary mechanism of fused glass densification generation during single particle scratching

Yueming Deng [a], Xiaoguang Guo [a], Hao Wang [a], Song Yuan [a,b], Wei Liu [a], Renke Kang [a], Shang Gao [a,*]

[a] State key laboratory of High-performance precision manufacturing, Dalian University of Technology, Dalian, 116024, China
[b] State Key Laboratory of Ultra-precision Machining Technology, The Hong Kong Polytechnic University, Hong Kong, China

ARTICLE INFO

Keywords:
Fused glass
Densification
Single particle scratching
ReaxFF MD
Environmental humidity

ABSTRACT

The densification of fused glass during processing has a significant impact on the performance and application of fused glass components. However, the precise atomic mechanisms underlying densification remain elusive. In this study, we explore the atomic mechanisms responsible for densification in fused glass during single particle scratching, with a focus on the scratching depths and environmental humidity. We employ reactive force field molecular dynamics (ReaxFF MD) simulations for our investigation. We subjected models to scratching under various humidity conditions using a spherical virtual indenter with a 20 Å radius. The scratching depths were set at 10 Å and 15 Å, respectively, with a constant scraping speed of 40 m/s. Our findings indicate that water molecules impede lateral atom movement on the fused glass surface while enhancing vertical flow. Furthermore, water molecules facilitate the volume recovery of fused glass following scratching. The transfer of hydrogen (H) atoms within the fused glass, facilitated by Si–O–H···O–Si structures, plays a crucial role in promoting volume recovery. The ultimate density distribution of fused glass results from a combination of atomic displacement during scratching and subsequent volume recovery. This study enhances our atomic-level understanding of densification generation in fused glass.

1. Introduction

Fused glass is widely used in high technology fields such as optics because of its excellent resistance to high temperature, acid corrosion and low coefficient of thermal expansion, as well as its good light transmission, specific and precise optical constants [1–4]. From a structural point of view, fused glass is a high purity amorphous silica material with a low atomic packing density [5]. The density of common α-quartz crystal is 2.65 g cm^{-3} [6], while the density of fused glass is only 2.20 g cm^{-3} [7], which makes large number of voids inside the fused glass [8]. At very high hydrostatic pressures, the density of fused glass increases significantly, producing densification [9–11]. As a high-performance specialty glass, fused glass components are often used in some extreme environments, such as high-power lasers [12], nuclear fusion [13], etc. However, the fused glass used in these fields needs to have excellent surface quality. The presence of densification after processing causes some physical properties of fused glass to change [14], which will seriously affect the optical performance stability of fused glass components and service life.

It is worth noting that densification during processing is not unique to fused glass, as many silica-based glass also can be densified during processing [9,15]. In fact, Yoshida et al. [16] have demonstrated that densification of glass materials under pressure shows a strong correlation between the densification of the glass material and the composition of the glass, and a strong correlation with the Poisson's ratio of the glass. Typically, the densification of fused glass occurs at a pressure of 2 GPa [17].Densification is divided into recoverable densification and non-recoverable densification [14]. Some studies found that the threshold for permanent densification of fused glass at hydrostatic pressure is 10 GPa by indentation tests, and at higher pressures, the maximum densification of fused glass is 20 % [8,18]. However, in scratching experiments, the threshold for permanent densification of the glass material is one order of magnitude lower than under hydrostatic pressure due to frictional forces [19]. Currently widely used fused glass processing methods, such as grinding, lapping, polishing, etc., involve the friction process during processing. This suggests that the threshold

* Corresponding author.
E-mail address: gaoshang@dlut.edu.cn (S. Gao).

https://doi.org/10.1016/j.jmrt.2023.11.269
Received 2 August 2023; Received in revised form 14 November 2023; Accepted 29 November 2023
Available online 2 December 2023

for densification of fused glass is much lower when these processing methods are used than when it is simply under pressure. Especially in the roughing stages, the larger forces and harder abrasive grains tend to locally reach the threshold of making fused glass to produce permanent densification. This requires a deeper study of the mechanism of densification generation in fused glass. Recently, scholars have paid more attention to the environmental influence on densification. Hojamberdiev et al. [20] studied the indentation recovery of soda lime silica glass (SLSG) under the coupling of different temperatures and ambient humidity and found that the indentation volume recovery was greater in high temperature and high humidity environments. They attributed this phenomenon to the thermal motion of atoms and the migration of alkaline ions, but this mechanism is not applicable to fused glass materials without alkaline ions. He et al. [21] found that the plastic deformation of the SLSG surface is strongly related to the relative humidity of the environment in which the glass is exposed by scratching experiment. However, they mainly explained the mechanism of densification from the perspective of macroscopic mechanical behavior, such as positive pressure and friction, and lack the analysis of microstructural level.

Due to the limitations of the testing equipment, the experimental detection of densification of glass material is commonly performed by heating the glass to the glass transition temperature after annealing [16], but this method has some disadvantages. Firstly, it can only be used to measure the volume recovery after densification, which cannot be measured in real-time. Secondly, this method can only detect the overall volume recovery of the densified region, but not the density distribution. In actual processing, there are uncertainties in the location and degree of local densification, and dynamic measurement is very difficult. Therefore, it is extremely difficult to investigate the mechanism of densification during processing in experiments. With the development of science and technology, computational power is constantly improving, and computational simulation can be a new way to study the densification mechanism. It is constrained by the uncertainty of the position and degree of local densification in actual processing, as well as the limitations of present testing equipment, despite the fact that there is a difference between the simulation and actual experimental scales, the MD simulations is still the greatest way to investigate how to induce densification during processing.Molecular dynamics (MD) [22,23], which can explain the mechanism of material removal during processing from the atomic scale, which is a computational method based on Newtonian mechanics. Using the molecular dynamics approach, several researchers have examined the friction and scratching of hard and brittle materials [24,25].Laser-induced densification of fused glass has been studied using MD [26] and the effect of densification on the mechanical behavior of fused glasses [27–29], such as fracture toughness and indentation, have also been extensively studied using MD.Du et al. [30] review the applications of first principles calculations, ab initio molecular dynamics simulations(AIMD), classical molecular dynamics (MD) simulations and kinetic Monte Carlo (KMC) simulations simulations to glass/water interactions and glass dissolution. Deng et al. [31]employed molecular dynamics simulations to investigate the sodium silicate glass and water interfacial reactions.

However, classical MD cannot observe the chemistry changes during processing. Bond order theory-based reactive force fields (ReaxFF) [32–35] has been successfully applied to MD simulations. This force field has been applied to several fields [36–39] and has shown great advantages especially in the fields of surface modification [40,41] and interfacial friction [42] at the atomic scale. Liu et al. [43] have used ReaxFF MD to investigate the influence of densification on the chemical mechanical polishing process at varied H_2O_2 concentrations, however they did not investigate the densification mechanism of molten glass at different scratch depths and ambient humidity.

In this paper, we utilized ReaxFF-MD to simulate the scratching process of fused glass with single particles and analyzed the mechanism of densification of fused glass under the coupling effect of scratching depths and environmental humidity. The study would focus on the contribution of water to the flow of atoms during scratching of fused glass and the contribution of volume recovery after scratching.

2. Model

We first modeled the quartz crystal (α-quartz) in Material Studio and then annealed it twice in Lammps [44,45] to obtain a model of the fused glass. The details of the annealing process were reported detailedly in previous studies [43,46–48]. During the first annealing process, the system was initially set at a temperature of 300 K. Subsequently, the system was heated to 4000 K under the NVT system synthesis and then gradually cooled back to the initial temperature. In the second annealing, the system underwent a reheating phase, reaching 4000 K under NPT system synthesis conditions at 1 atm pressure (0.1 MPa), followed by a 50 ps hold, and concluded with a gradual cooling back to the initial temperature. The rate of all warming and cooling processes was 25 K/ps. All visualization work of the models was carried out in OVITO [49]. The size of the model of ideal fused glass was 107.25 Å × 67.09 Å × 55.23 Å, and contained a total of 28080 atoms with an average density of 2.24 g cm^{-3}, which was very close to the density of the actual fused glass produced [25].

Reacting different amounts of water molecules with the surface of fused glass for 200ps to study the evolution of densification of fused glass in low, medium and high humidity environments. The number of water molecules and the detailed parameters of the models were shown in Table 1. The models in different humidity environments were scratched by using a spherical virtual indenter with a radius of 20 Å. The X-axis, Y-axis and Z-axis of the centroid coordinates of the virtual indenter are 130 Å, 30 Å and 70.23 Å, respectively. Scratch from the rightmost center of the workpiece (the Y-axis position of the model was 30 Å) along the negative direction of the X-axis at a speed of 40 m/s. Higher scratch speed is widely used in MD due to the limitation of computing level [50,51]. The depths of scratching were 10 Å and 15 Å, which were used to investigate the effect of scratching depths on densification, as shown in Fig. 1. The virtual indenter's centroid first descends along the Z-axis to a specified depth before beginning to scratch, and it then scrapes at a specified depth along the X-axis's negative direction. The model used periodic boundary conditions in the Y-direction and non-periodic boundary conditions in the X-direction and Z-direction, and used reflection walls to prevent atoms loss [52]. The scratching model was divided into a fixed layer, a thermostatic layer and a Newton layer. The fixed layer was used to fix the model and prevent the influence of boundary effects on the model. Heat energy was transferred between the thermostatic layer and the Newton layer, and the Newton layer did not control the temperature, which conformed to Newton's law of motion.

NVT ensemble was applied to the simulation process of the model, and the thermostatic layer was controlled at 300K using the Berendsen temperature control method [53]. The timestep was set to 0.1fs [54] Withdraw the virtual indenter after scratching. And then, the whole model was relaxed 50ps at 300K temperature to fully recover the deformation during the scratching process. The Si/O/H potential function developed by Fogarty et al. [33] was used in the entire simulation

Table 1
Modeling parameters of fused glass scratching model.

Parameter	Preset conditions
Size of fused glass	107.25 Å × 67.09 Å × 55.23 Å
Average density of fused glass	2.24 g cm^{-3}
Virtual indenter radius	20 Å
Depth of scratching	10 Å, 15 Å
Speed of scratching	40 m/s, negative direction along X-axis
Distance of scratching	80 Å
Number of water molecules	0, 800, 2400, 4000
Timestep	0.1fs

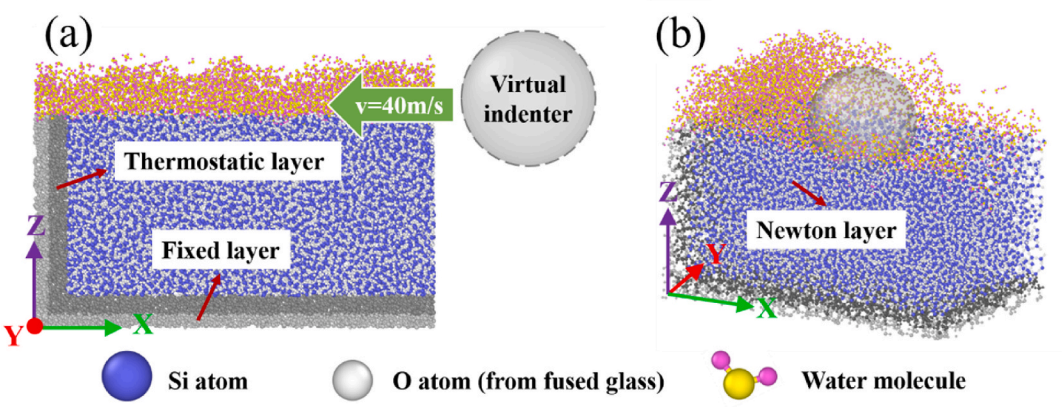

Fig. 1. Fused glass scratching model (a) before scratching, front view, (b) in the process of scratching, 3D-view.

process, which had been proved to be able to simulate the chemical reaction between amorphous silica and water at the interface with relatively high accuracy and was excellent agreement with quantum mechanical data in terms of structural information, chemical and electrical properties of the interface.

As we utilized a virtual indenter for scratching, the entire system exclusively encompassed the chemical interaction between fused glass and H2O, with the indenter remaining uninvolved in the chemical reactions.

3. Results and discussion

3.1. The density distribution and volume recovery after scratching

We calculated the density of fused glass using the slice statistics method, as shown in Figs. 2 and 3. Firstly, we compared the density change of fused glass under dry environment and high humidity environment after fully reacting with water molecules, and found that the reaction of water molecules on the surface of fused glass had almost no effect on the density of fused glass, as shown in Fig. 2. Therefore, we use the density data under dry condition as the control group (Initial Value) for the simulation in the next comparison of density changes after scratching.

At the scratching depth of 10 Å, as shown in Fig. 3(a) and (c), significant densification areas are visible in the range of 5~17.5 Å (7.5–17 Å in a dry environment) from the model's top surface. After scratching the fused glass can be roughly divided into four regions according to the density distribution, as shown in Fig. 3(c). The bottom layer is the undeformed fused glass substrate with almost constant density; then there is the plastic deformation region where the density deviates from the initial value but does not increase significantly relative to the density before scratching; further up is the densification layer with significant density increase; and the uppermost layer is the scratching layer, where the atoms flow around the indenter due to the virtual indenter. Similarly, at the scratching depth of 15 Å, as shown in Fig. 3(b), significant densification areas are visible in the range of 7.5–26.5 Å (12.5–28.5 Å in a dry environment) from the model's top surface.And a deformation layer exists in the region of 26.5–34.5 Å from the top surface of the model. By comparing the thickness of the densification region and the plastic deformation region, it is easy to find that the two regions are thicker at the scratching depth of 15 Å. This indicates that a larger scratching depth can cause a thicker densification layer and a thicker plastic deformation layer.

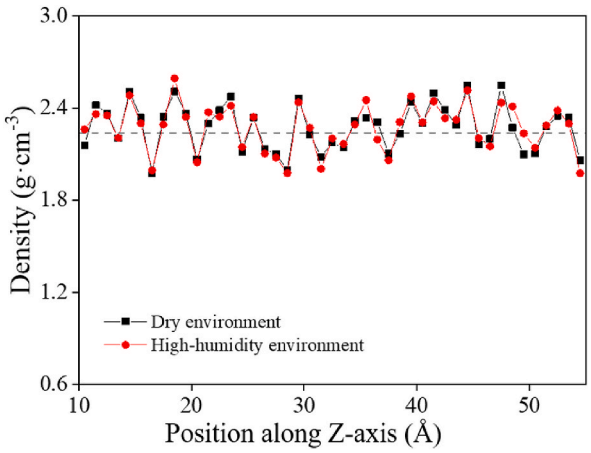

Fig. 2. Density distribution of fused glass in the relaxation phase. The gray dashed line in the figure indicates the average density of fused glass.

It is evident that under all conditions, the thickness of the densification region in the Z-axis of the fused glass, following adequate relaxation, is smaller than the indentation depths (45 Å for a scratching depth of 10 Å and 40 Å for a scratching depth of 15 Å). In simpler terms, the bottom of the scratching region rests higher than the bottom of the virtual indenter after scratching, signifying a degree of volume recovery during the fused glass's relaxation. Moreover, irrespective of the scratching depths, the point at which the fused glass density notably decreases under dry conditions is lower than that under wet conditions. This suggests that volume recovery in fused glass is more effective in humid environments. To visually represent the volume recovery of the fused glass, we tracked the change in the position of the lowest point of the glass scratches during and after scratching, as depicted in Fig. 4. Directly quantifying volume changes is challenging. It is evident that the volume recovery of fused glass increases with rising ambient humidity, irrespective of the scratching depths. This demonstrates that the presence of water molecules indeed promotes the recovery of volume in the non-permanently densified fused glass after scratching. Mirabbos et al. [20] also found in their indentation tests that the indentation recovery rate of glass materials was greater in a 100 % relative humidity environment than in a room temperature/room humidity, which justified the conclusions of our simulations. It is also worth noting that under dry conditions, the volume recovery of the scratching depth of 15 Å is smaller than that of the scratching depth of 10 Å, which indicates that more irrecoverable densification occurs when the scratching depth is 15 Å.

3.2. The displacement of atoms during scratching

We counted the displacement of atoms in the surface (Y-direction) and in the vertical direction (Z-direction) for fused glass under various conditions. And colored the atoms with different displacements and plotted the clouds as shown in Fig. 5 ~8, where the negative signs

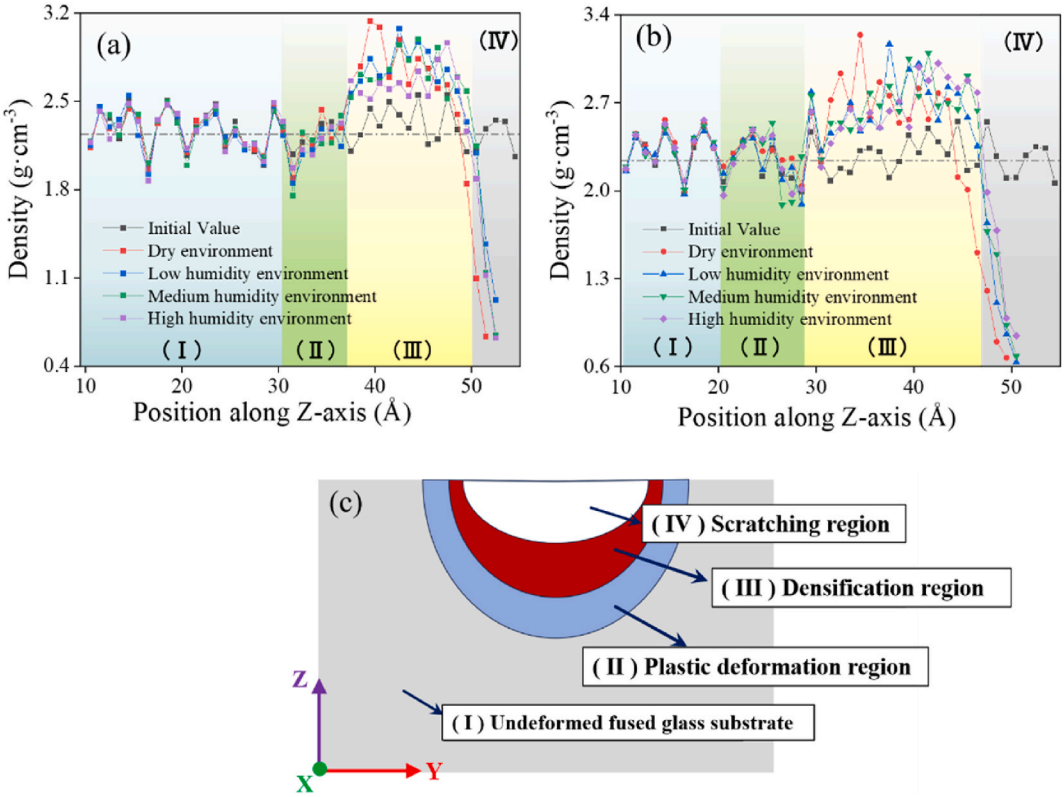

Fig. 3. Density distribution of fused glass after scratching, (a) density distribution after scratching with the scratching depth of 10 Å, (b) density distribution after scratching with the scratching depth of 15 Å, (c) division of each region and various regions of fused glass after scratching. In the figure, (I) indicates the undeformed fused glass substrate, (II) indicates the plastic deformation region, (III) indicates the densification region, and (IV) indicates the scratching region. The gray dashed line in the figure indicates the average density of fused glass.

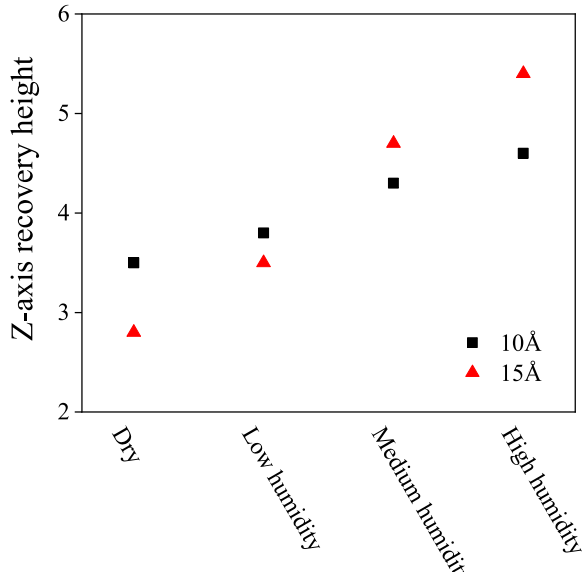

Fig. 4. Volume recovery of fused glass after scratching under different conditions.

indicate the direction of displacement.

Figs. 5 and 6 show the displacement of atoms in the three-dimensional space in the XY plane, and the scratch depth is 10 and 15 Å respectively in different humidity environments. The positive direction of the Y axis is the positive direction of the displacement direction, and the negative direction of the Y axis is the negative direction of the displacement direction. As can be seen in Figs. 5 and 6, in the dry environment, the number of atoms possessing larger displacements (5 Å) is higher. As the ambient humidity increases, the number of atoms possessing larger displacements decreases. The phenomena described above indicate that H_2O has an inhibitory effect on the displacement of atoms in fused glass.

Figs. 7 and 8 are able to further observe the distribution of the atomic displacements. To facilitate observation, we marked atoms with displacements less than 3 Å as gray, and showed only atoms in the region of 22.5–47.5 Å in the Z-axis direction for the scratching depth of 15 Å, and only atoms in the region of 25~45 Å in the Z-axis for the scratching depth of 10 Å, as shown in Figs. 7 and 8. It can be seen that, regardless of the conditions, the atoms with the largest displacement are concentrated in the surface layer scratched by the virtual indenter, and the further down the layer, the smaller the displacement of the atoms. In addition, as the area circled in Fig. 8, the volume recovery of the atom has clearly appeared. With the increase of ambient humidity, atoms with greater displacement show a tendency to decrease and then increase. This is because fused glass in the dry environment has a very limited ability to recover volume due to the lack of facilitation of volume recovery by water molecules. As the environmental humidity increases, although the capacity for volume recovery increases, the displacement of atoms also increases. So that some of the atoms with large displacements also appear at higher environmental humidity. This phenomenon indicates, on the one hand, the contribution of water molecules to the volume recovery of fused glass after scratching and, on the other hand, the final density distribution of fused glass as a result of the combined effect of atomic displacement and volume distribution.

3.3. Bond order changes during relaxation and scratching

Water molecules can change the surface properties of fused glass

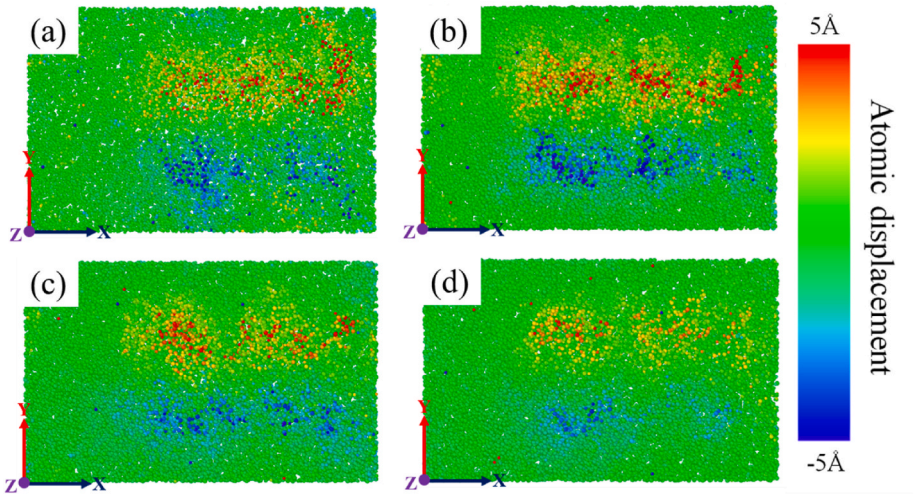

Fig. 5. Atomic displacement flow on the surface of fused glass during scratching at the scratching depth of 15 Å, (a) dry environment, (b) low humidity environment, (c) medium humidity environment, (d) high humidity environment.

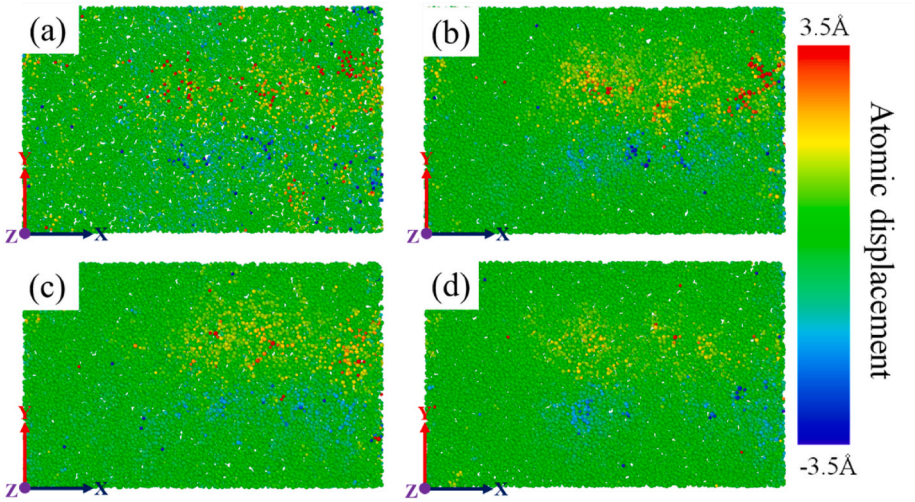

Fig. 6. Atomic displacement flow on the surface of fused glass during scratching at the scratching depth of 10 Å (a) dry environment, (b) low humidity environment, (c) medium humidity environment, (d) high humidity environment.

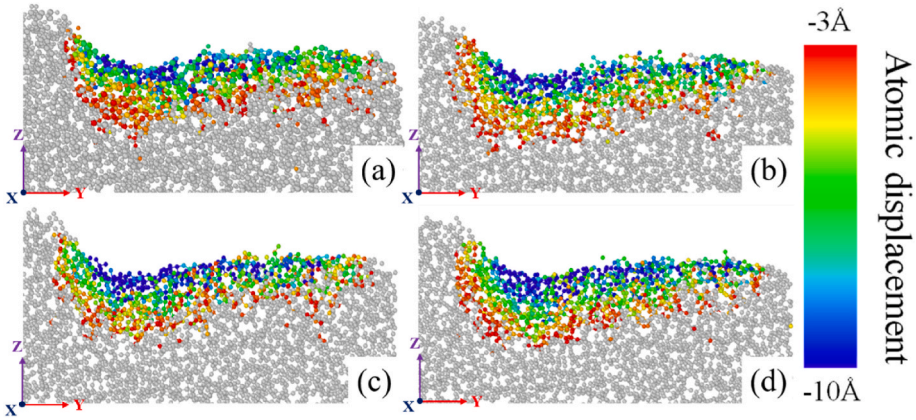

Fig. 7. Atomic displacement in the vertical direction of fused glass during scratching at the scratching depth of 15 Å, (a) dry environment, (b) low humidity environment, (c) medium humidity environment, (d) high humidity environment.

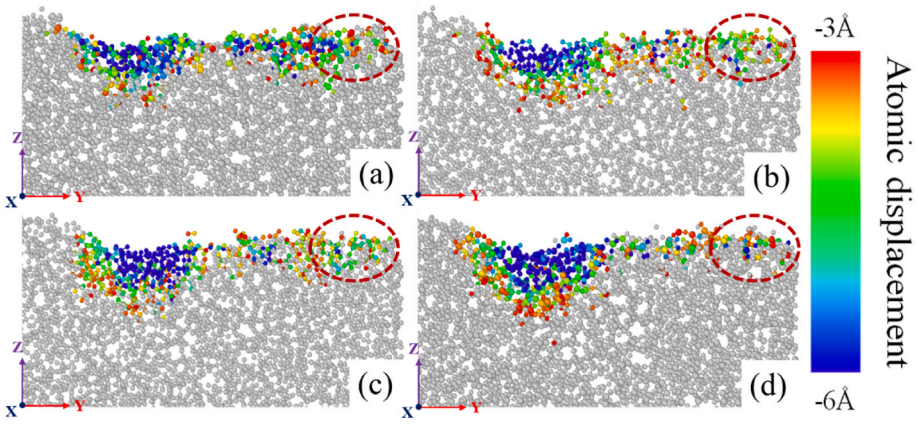

Fig. 8. Atomic displacement in the vertical direction of fused glass during scratching at the scratching depth of 10 Å, (a) dry environment, (b) low humidity environment, (c) medium humidity environment, (d) high humidity environment.

[46], so that the atomic displacement of fused glass in the surface and vertical directions exhibits reduce attenuation trends with the increase of ambient humidity. According to previous experience, the reaction depths of fused glass surface with water is about 5 Å [46]. Therefore, we counted the bond order of Si–O bonds in the region above 50 Å of the z-axis (hereinafter referred to as the surface region, and the Si–O bonds in this region include the Si–O bonds in the fused glass substrate and in the generated Si–OH bonds.) and at the region from 45 to 50 Å, as shown in Fig. 9.

In the surface region, the average bond order increases gradually with the increase of environmental humidity. For covalent bonds, the larger the bond order between atoms, the stronger the covalent bonds, the more stable the covalent bonds, and the greater the energy required to break the covalent bonds. Therefore, as the ambient humidity increases, the energy required to make changes in the surface structure during scratching of fused glass also increases, resulting in a decreasing of the atomic displacement in the surface region. Below the surface region the bond order in the 45–50 Å region is always in dynamic equilibrium within a certain range and does not change with the environmental humidity. This indicates that the effect of water on fused glass is only on the surface, and there is no significant effect on the inside

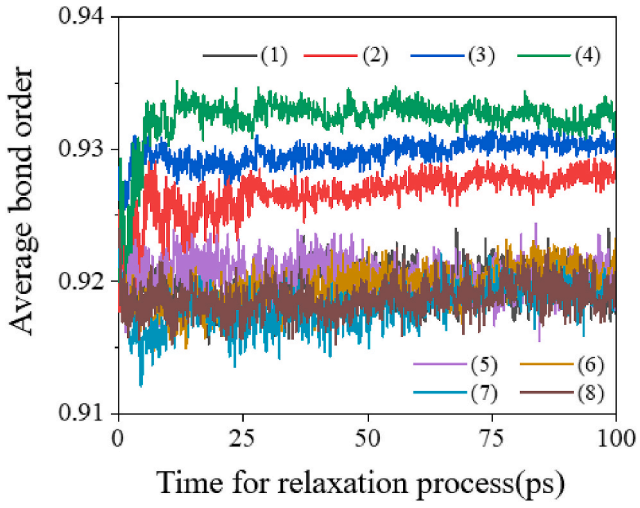

Fig. 9. Bond order of Si–O bonds in the surface region (region above 50 Å) and 45–50 Å region of fused glass during relaxation in different conditions, in which (1) ~ (4) are surface regions, in order of dry environment, low humidity environment, medium humidity environment and high humidity environment, and (5) ~ (8) are 45–50 Å regions, in order of dry environment, low humidity environment, medium humidity environment and high humidity environment.

of fused glass. However, the both scratching depths we set are greater than 10 Å.

In order to study the mechanism of action of the effect of water molecules on the atomic displacement of fused glass in the vertical plane, we calculated the forces on the virtual indenter during the scratching, As shown in the Fig. 10. It can be seen that as the ambient humidity increases, the positive pressure on the fused glass during the scratching increases. However, the effect of ambient humidity is less than the effect of scratching depth. The atoms in the fused glass substrate are more displaced by larger forces, resulting in increased atomic displacement in the vertical direction. The force on the virtual indenter increases with scratching, which is probably caused by the increasing accumulation of atoms under the indenter.

During the scratching process, we counted the bond order in a certain depth region below the virtual indenter under different conditions, as shown in Fig. 11. At first, only the average bond order of the rightmost 40 Å × 40 Å region of the fused glass is counted, and when the virtual indenter is completely inside the fused glass substrate, the counted area follows the movement of the virtual indenter, and the specific depths are the depths of the bottom layers of the densification regions shown in the Fig. 3. It can be seen that when the depth of scratching is small, Fig. 11 (a), the bond order of Si–O bonds below the indenter is reduced. Under dry conditions, the bond order of fused glass decreases insignificantly, but as the environmental humidity increases, the bond order of fused glass decreases gradually. At a larger depth of scratching, Fig. 11(b), the bond order also exhibits a decreasing trend with increasing environmental humidity, and the decrease is larger than that at the scratching depth of 10 Å. This observation implies that with increasing environmental humidity, the influence of the virtual indenter on the internal substrate of the fused glass intensifies during scratching, aligning with the previously discussed variation in positive pressure with humidity. Consequently, this results in a reduction in the bond order of the fused glass, thereby facilitating atomic movement of the fused glass in the vertical direction.

3.4. Change in the amount of Si–OH at the scratch area

The reaction of fused glass surface with H_2O to form Si–OH has been extensively studied [47,55,56]. However, Si–OH at the scratches has rarely been studied. In fact, the fused glass substrate at the scratched area is still capable of hydroxylation when exposed to a humid environment after scratching, As shown in Fig. 12. Low levels of ambient humidity result in low levels of Si–OH production. As the environmental humidity increases, the number of water molecules reacting with the scratched surface increases, and the amount of Si–OH generated increases. When the depths of the scratch increase, the amount of Si–OH

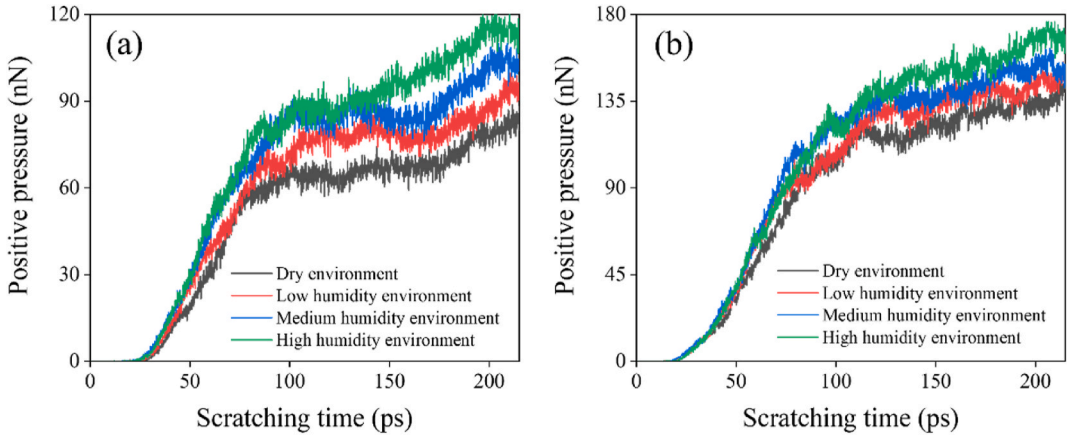

Fig. 10. Positive pressure during scratching, (a) the scratching depth of 10 Å, (b) the scratching depth of 15 Å.

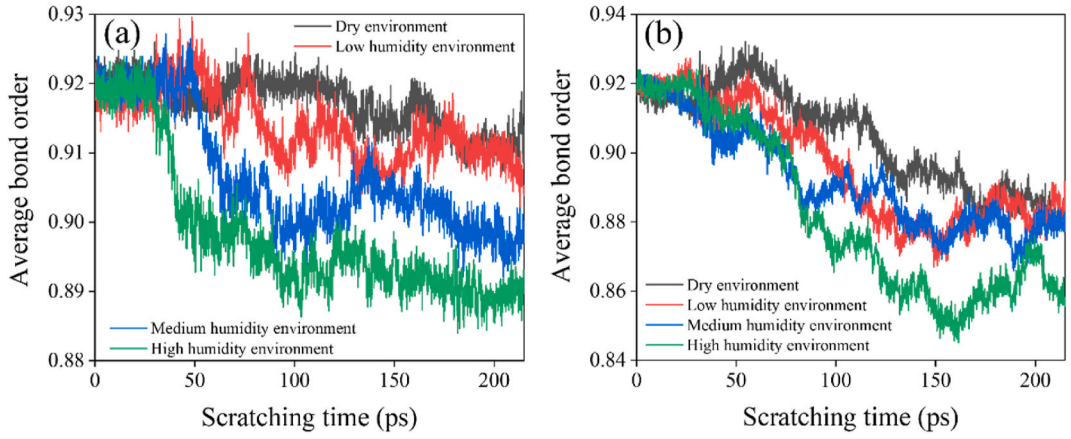

Fig. 11. Bond order of Si–O bonds in the region below the virtual indenter during scratching, (a) the scratching depth of 10 Å, (b) the scratching depth of 15 Å.

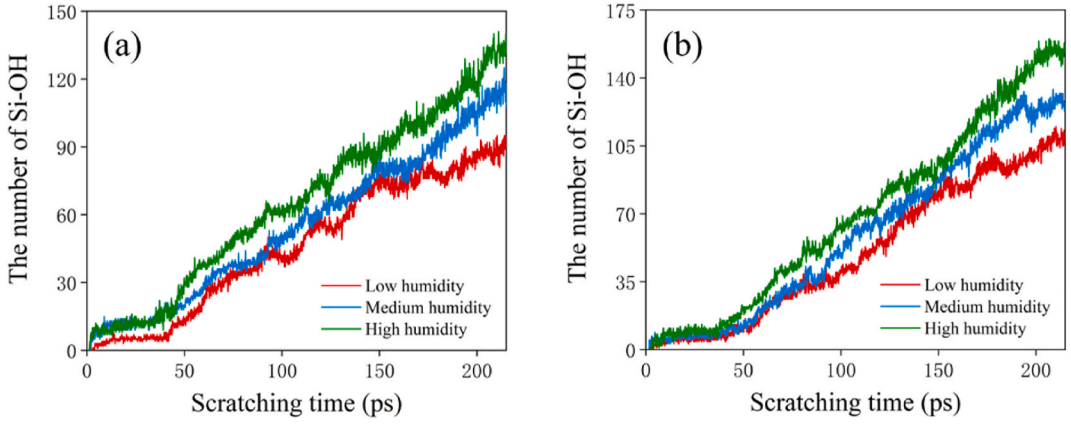

Fig. 12. The amount of Si–OH generated at the scratch during the scratching process (a) scratching depth of 10 Å, (b) scratching depth of 15 Å.

generated also increases, because the area at the scratches also increases when the scratching depth is larger, and the area for reaction with water molecules increases. Du et al. [57] found that the level of surface hydroxylation of fused glass was 4.5/nm^2. We calculated the surface hydroxyl concentration at the final scratches, as shown in Fig. 13. It can be seen that although the number of hydroxyl is higher when the scratching depth is 15 Å, the concentration of hydroxyl in the per unit area decreases. This is perhaps due to the hindering effect of densification on the hydroxylation of the fused glass surface [43].

3.5. Process of H transfer inside fused glass

In section 3.1 we have found that water has a facilitating effect on the volume recovery of fused glass after scratching. This indicates that there are "facilitating factors" to accelerate the structural change of fused glass in the environment containing water molecules. It has been found that the migration of alkaline ions in SLSG can promote the volume recovery of the indentation of SLSG [20]. Alkaline ions are the "promoting factors" of SLSG. However, in our fused glass simulation system

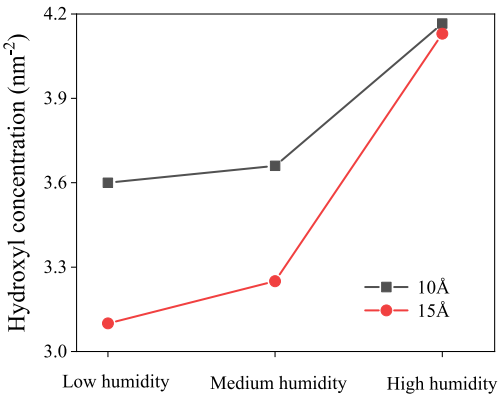

Fig. 13. Hydroxylation concentration under different conditions.

no alkaline ions are present, and only water molecules are present. The "facilitation factors" obviously come from water molecules. We focused our studies on the H atoms and followed the relaxation process after scratching, because study has found that H can penetrate inside fused glass [43,46].

We followed the transfer of H atoms and took atomic snapshots, and found that in different conditions, the downward transfer of H atoms relies on the Si–O–H···O–Si structure, which promotes a change in the structure of fused glass. For ease of observation, we have removed some of the atoms and grayed out the irrelevant ones and the green O in the figure comes from the quartz glass substrate and the yellow O comes from the water molecules (same as below). In order to more clearly describe the transfer process of hydrogen atoms inside the molten glass, the adjacent silicon dioxide molecules were labeled, Si^1, O^1, Si^2 and O^2 respectively represent the silicon atoms and oxygen atoms on the SiO_2.

Fig. 14 illustrates the way in which the H atom forms Si–O–H···O–Si directly with the incompletely coordinated O atom. At the 224.6ps moment, the H inside the fused glass forms the Si^2–O^2H structure with Si^2 and O^2, and O^1 is connected to the surrounding atoms Si^1 by the same bond as Si^2–O^2, as shown in Fig. 14(a). O^2 is in the undercoordinated state. After 0.2ps, in Fig. 14(b), H is attached to O^2, forming the Si^1–O^1–H···O^2–Si^2 structure. The Si–O–H···O–Si structure is extremely unstable and breaks after only 0.5ps, in Fig. 14(c).

In addition to direct transfer, H atoms are also transferred in the form of breaking Si–O–Si bonds. Fig. 15 illustrates the way in which the Si–O–Si bond is first broken and then Si–O–H···O–Si is formed. At the 144.8ps moment, there are Si^1–O^1H structure and Si^2–O^2–Si^3 structure in the system, as shown in Fig. 15(a). After 0.4ps, Si^2–O^2–Si^3 breaks and Si^2–O^2 forms Si^1–O^1–H···O^2–Si^2 structure with Si^1–O^1H, Fig. 15(b). At the moment of 156ps, the Si^1–O^1–H···O^2–Si^2 structure breaks and the H atom is transferred to the Si^2–O^2H structure, in Fig. 15(c). Fig. 16, on the other hand, shows the transfer of the H atom to form a special structure before breaking the Si–O–Si bond. At the moment of 162.4ps, there exists Si^1–O^1–Si^2 structure and Si^3–O^2H structure as shown in Fig. 16(a). After 0.2ps, Si^1–O^1–Si^2 is not directly disconnected, but forms a special structure with Si^3–O^2H as shown in Fig. 16(b). After that, the Si^2–O^1 bond is broken and the O^2–H bond is also broken to form the Si^1–O^1–H structure, and the O^2 and Si^2 are connected into a bond to form the Si^2–O^2–Si^3 structure, in Fig. 16(c). It is noteworthy that the bridge bond O^2 atom in Si^2–O^2–Si^3 comes from the water molecule, which indicates that O from the water molecules is involved in the composition of the fused glass structure during the transfer of H atoms.

4. Conclusions

We employed the ReaxFF-MD method to simulate the scratching process of ideal fused glass. Our investigation included the study of densification under various scratching depths and environmental humidity conditions. We conducted a comprehensive analysis of how environmental humidity impacts atomic displacement during scratching and the subsequent volume recovery of the fused glass. The ultimate density distribution in the fused glass is determined by the interplay between atomic displacement during scratching and the subsequent volume recovery. The main conclusions of the study are as follows:

(1) In the absence of external forces, natural environmental humidity has minimal impact on the density of fused glass. Following scratching, fused glass exhibits volume recovery, with water molecules playing a key role in promoting this process. Consequently, higher environmental humidity levels result in more substantial volume recovery.

(2) During scratching, atomic displacement induced by the mechanical action of the virtual indenter occurs in the fused glass. Deeper scratch depths result in more pronounced displacement of the fused glass in various directions. With increasing environmental humidity, the displacement of fused glass on the surface decreases in the lateral direction but intensifies in the vertical direction. This suggests that H_2O inhibits atomic displacement of fused glass on the surface while promoting it vertically.

(3) During the relaxation process, the interaction of fused glass with water leads to an increase in bond order on the surface, signifying the strengthening of Si–O bonds. However, the bond order in the subsurface region remains largely unaffected, indicating that, under natural conditions, water primarily impacts surface bond order. This effect inhibits atomic displacement on the surface of the fused glass during subsequent scratching. However, during the scratching process, higher environmental humidity leads to increased force on the virtual indenter and a reduction in the bond order of fused glass beneath the virtual indenter. This elucidates that the heightened interaction between the virtual indenter and the fused glass substrate promotes the vertical flow of fused glass atoms during scratching.

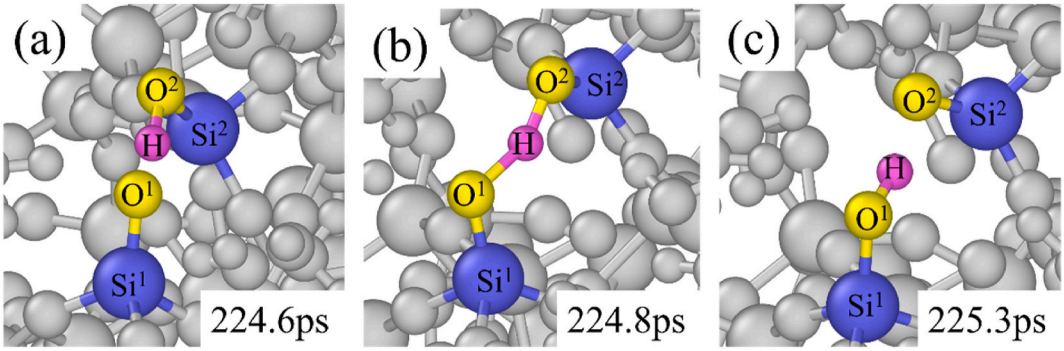

Fig. 14. Direct transfer form of H.

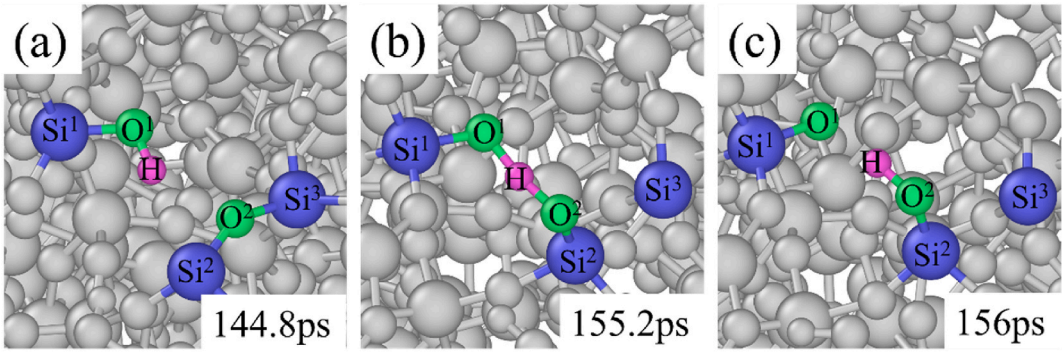

Fig. 15. The transfer form of Si–O–Si bond is broken first.

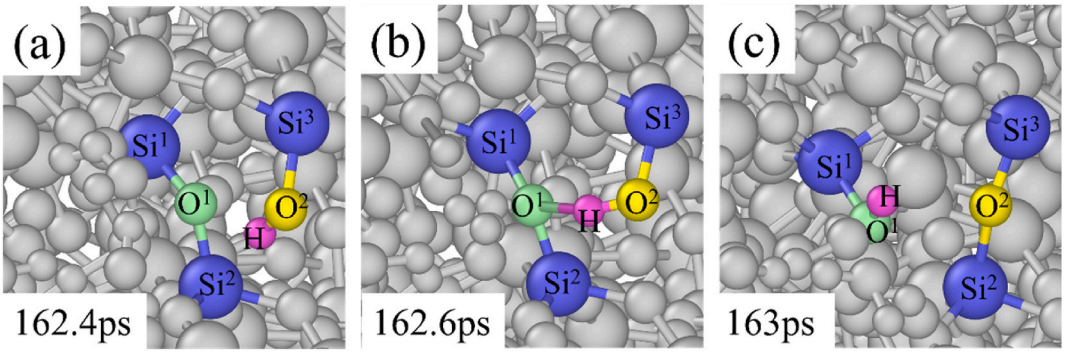

Fig. 16. Transfer form of H atoms to form the special structure.

(4) In the course of the volume recovery process, hydrogen (H) within the fused glass undergoes transfer via the Si–O–H···O–Si structure, which, in turn, facilitates structural alterations in the fused glass. By tracking and observing this process, we identified three distinct forms in which hydrogen (H) atoms contribute to the formation of the Si–O–H···O–Si structure: (a) H atoms directly bond with undercoordinated oxygen (O) atoms, resulting in the formation of the Si–O–H···O–Si structure. (b) H atoms create the Si–O–H···O–Si structure by breaking one of the Si–O bonds in the Si–O–Si structure. (c) H atoms bond with fully coordinated oxygen (O) atoms, resulting in the formation of the distinctive structure depicted in Fig. 16(b), leading to the rupture of Si–O bonds.

(5) The final density distribution of the fused glass after scratching is the result of a combination of atomic displacement during scratching and volume recovery after scratching. While water molecules play a role in both atomic displacement and volume recovery, their impact on densification is comparatively less pronounced than the effect of scratching depths.

Credit authors statement

Yueming Deng: Investigation, Methodology, Writing - original draft, Visualization. **Xiaoguang Guo:** Writing - review & editing, Supervision, Funding acquisition, Resources. **Hao Wang:** Investigation, Formal analysis, Writing - review & editing. **Song Yuan:** Writing - review & editing. **Wei Liu:** Writing - Review & Editing. **Renke Kang:** Supervision, Project administration. **Shang Gao:** Conceptualization, Writing - Review & Editing.

Statement of originality

No conflict of interest exists in the submission of this manuscript, and the manuscript is approved by all authors for publication. I would like to declare on behalf of my co-authors that the work described was original research that has not been published previously, and not under consideration for publication elsewhere, in whole or in part. All the authors listed have approved the manuscript that is attached.

Declaration of competing interest

The authors declare that they have no known competing financial interests or personal relationships that could have appeared to influence the work reported in this paper.

Acknowledgements

The authors greatly appreciate the financial support of the National Key Research and Development Program of China (2022YFB3404304), the National Natural Science Foundation of China (51991371), and the National Key Research and Development Program of China (2022YFB360016202). The authors also acknowledge the Beijing Super Cloud Computing Center (BSCC) for providing HPC resources that have contributed to the research results reported within this paper.

References

[1] Piramanayagam SN, Srinivasan K. Recording media research for future hard disk drives. J Magn Magn Mater 2009;321(6):485–94.
[2] Chu C, Pan M. Effective thermal emission on TFT–LCD TV panels for improving image quality. Adv Eng Software 2010;41(2):130–40.
[3] Yu Y, et al. Shifting selectivity of collinear volume holographic storage. Opt Commun 2010;283(20):3895–900.
[4] Joodaki M, Kompa G. Application of neural networks for extraction of distance and reflectance in pulsed laser radar. Measurement 2007;40(6):724–36.
[5] Funamori N, Sato T. Sixfold-coordinated amorphous polymorph of SiO2 under high pressure. Phys Rev Lett 2008;101(25):255502.
[6] Levien L, Prewitt CT, Weidner DJ. Structure and elastic properties of quartz at pressure. Am Mineral 1980;65(9–10):920–30.
[7] Ji H, et al. Poisson's ratio and the densification of glass under high pressure. Phys Rev Lett 2008;100(22):225501.

[8] Li C, et al. A finite element study on the effects of densification on fused silica under indentation. Ceram Int 2020;46(17):26861–70.
[9] Lee KH, et al. Atomic-scale mechanisms of densification in cold-compressed borosilicate glasses. J Am Ceram Soc 2021;104(6):2506–20.
[10] Shorey A, et al. Deformation of fused silica: nanoindentation and densification. 1998. p. 3424.
[11] Christiansen EB, Kistler SS, Gogarty WB. Irreversible compressibility of silica glass as a means of determining the distribution of force in high-pressure cells. J Am Ceram Soc 1962;45(4):172–7.
[12] Wuest P, et al. Fused silica fast axis collimator lens for blue high-power laser diodes. 2019, 10899.
[13] Yan Y, He J. Design of optical system for fusion reaction-rate measurement. Opt Precis Eng 2012;20(11):2389.
[14] Piao F, Oldham WG, Haller EE. The mechanism of radiation-induced compaction in vitreous silica. J Non-Cryst Solids 2000;276(1):61–71.
[15] Rouxel T, Jang J, Ramamurty U. Indentation of glasses. Prog Mater Sci 2021;121:100834.
[16] Yoshida S, Sanglebœuf J, Rouxel T. Quantitative evaluation of indentation-induced densification in glass. J Mater Res 2005;20(12):3404–12.
[17] Bruns S, et al. Indentation densification of fused silica assessed by Raman spectroscopy and constitutive finite element analysis. J Am Ceram Soc 2020;103(5):3076–88.
[18] Yoshida S. Indentation deformation and cracking in oxide glass –toward understanding of crack nucleation. J Non-Cryst Solids X 2019;1:100009.
[19] He H, et al. Friction-induced subsurface densification of glass at contact stress far below indentation damage threshold. Acta Mater 2020;189:166–73.
[20] Hojamberdiev M, Stevens HJ, LaCourse WC. Environment-dependent indentation recovery of select soda-lime silicate glasses. Ceram Int 2012;38(2):1463–71.
[21] He H, et al. Effect of humidity on friction, wear, and plastic deformation during nanoscratch of soda lime silica glass. J Am Ceram Soc 2022;105(2):1367–74.
[22] He M, Joshi K, Zhigilei LV. Computational study of the effect of core–skin structure on the mechanical properties of carbon nanofibers. J Mater Sci 2021;56(26):14598–610.
[23] Lelièvre T, Stoltz G. Partial differential equations and stochastic methods in molecular dynamics. Acta Numer 2016;25:681–880.
[24] Li C, et al. Understand anisotropy dependence of damage evolution and material removal during nanoscratch of MgF2 single crystals. Int J Extrem Manuf 2023;5.0151011.
[25] Y S. Fabrication technology and quality factor improvement for fused silica Micro Hemispherical Resonator. National University of Defense Technology; 2021.
[26] Kubota A, et al. Densification of fused silica due to shock waves and its implications for 351 nm laser induced damage. Opt Express 2001;8(11):611–6.
[27] Liang Y, Miranda CR, Scandolo S. Mechanical strength and coordination defects in compressed silica glass: molecular dynamics simulations. Phys Rev B 2007;75(2):024205.
[28] Hu Z, et al. Atomistic study on tensile fracture of densified silica glass and its dependence on strain rate. Chin Phys B 2020;29(12):128101.
[29] Liu C, et al. Molecular dynamics simulation on structure evolution of silica glass in nano-cutting at high temperature. Mol Simulat 2020;46(13):957–65.
[30] Du J, Rimsza JM. Atomistic computer simulations of water interactions and dissolution of inorganic glasses. npj Mater Degrad 2017;1(161).
[31] Deng L, et al. Ion-exchange mechanisms and interfacial reaction kinetics during aqueous corrosion of sodium silicate glasses. npj Mater Degrad 2021;5(151).
[32] Chenoweth K, Van Duin AC, Goddard WA. ReaxFF reactive force field for molecular dynamics simulations of hydrocarbon oxidation. J Phys Chem 2008;112(5):1040–53.
[33] Fogarty JC, et al. A reactive molecular dynamics simulation of the silica-water interface. J Chem Phys 2010;132(17):174704.
[34] Martini A, Eder SJ, Dörr N. Tribochemistry: a review of reactive molecular dynamics simulations. Lubricants 2020;8(4):44.
[35] Dongol R, et al. Molecular dynamics simulation of sodium aluminosilicate glass structures and glass surface-water reactions using the reactive force field (ReaxFF). Appl Surf Sci 2018;439:1103–10.
[36] Mao Q, et al. Cost-effective carbon fiber precursor selections of polyacrylonitrile-derived blend polymers: carbonization chemistry and structural characterizations. Nanoscale 2022;14(17):6357–72.
[37] Rajabpour S, et al. Low-temperature carbonization of polyacrylonitrile/graphene carbon fibers: a combined ReaxFF molecular dynamics and experimental study. Carbon 2021;174:345–56.
[38] Rimsza JM, et al. Water interactions with Nanoporous silica: comparison of ReaxFF and ab initio based molecular dynamics simulations. J Phys Chem C 2016;120(43):24803–16.
[39] Liu J, et al. Reaction analysis and visualization of ReaxFF molecular dynamics simulations. J Mol Graph Model 2014;53:13–22.
[40] Yuan S, et al. Insights into the surface oxidation modification mechanism of nano-diamond: an atomistic understanding from ReaxFF simulations. Appl Surf Sci 2021;540.
[41] Rajabpour S, et al. Development and applications of ReaxFF reactive force fields for group-III Gas-phase Precursors and surface reactions with graphene in Metal–Organic chemical Vapor Deposition synthesis. J Phys Chem C 2021;125(19):10747–58.
[42] Yuan S, et al. Effects of pressure and velocity on the interface friction behavior of diamond utilizing ReaxFF simulations. Int J Mech Sci 2021;191:106096.
[43] Liu W, Yuan S, Guo X. Atomic understanding of the densification removal mechanism during chemical mechanical polishing of fused glass. Appl Surf Sci 2022;591:153166.
[44] Plimpton S. Fast parallel algorithms for short-range molecular dynamics. J Comput Phys 1995;117(1):1–19.
[45] Aktulga HM, et al. Parallel reactive molecular dynamics: Numerical methods and algorithmic techniques. Parallel Comput 2012;38(4–5):245–59.
[46] Guo X, et al. Study using ReaxFF-MD on the CMP process of fused glass in pure H2O/aqueous H2O2. Appl Surf Sci 2021;556:149756.
[47] Guo X, et al. Effect of surface hydroxylation on ultra-precision machining of quartz glass. Appl Surf Sci 2020;501:144170.
[48] Rimsza JM, Jones RE, Criscenti LJ. Surface structure and stability of Partially hydroxylated silica surfaces. LangmuirLangmuirLangmuir 2017;33(15):3882–91.
[49] Stukowski A. Visualization and analysis of atomistic simulation data with OVITO–the Open Visualization Tool. Model Simulat Mater Sci Eng 2009;18(1):015012.
[50] Li P, et al. Effects of grinding speeds on the subsurface damage of single crystal silicon based on molecular dynamics simulations. Appl Surf Sci 2021;554:149668.
[51] Liu T, et al. Study on the surface damage layer in Multiple grinding of quartz glass by molecular dynamics simulation. J Nano Res 2017;46:192–202.
[52] Assowe O, et al. Reactive molecular dynamics of the initial oxidation stages of Ni (111) in pure water: effect of an applied electric field. J Phys Chem 2012;116(48):11796–805.
[53] Berendsen HJC, et al. Molecular dynamics with coupling to an external bath. J Chem Phys 1984;81(8):3684–90.
[54] Deng L, et al. Reaction mechanisms and interfacial behaviors of sodium silicate glass in an aqueous environment from reactive force field-based molecular dynamics simulations. J Phys Chem C 2019;123(35):21538–47.
[55] Guo X, et al. Effects of pressure and slurry on removal mechanism during the chemical mechanical polishing of quartz glass using ReaxFF MD. Appl Surf Sci 2020;505:144610.
[56] Hahn SH, van Duin ACT. Surface Reactivity and Leaching of a sodium silicate glass under an aqueous environment: a ReaxFF molecular dynamics study. J Phys Chem C 2019;123(25):15606–17.
[57] Du J, Cormack AN. Molecular dynamics simulation of the structure and hydroxylation of silica glass surfaces. J Am Ceram Soc 2005;88(9):2532–9.